Chaos, Solitons and Fractals 157 (2022) 111972

Contents lists available at ScienceDirect

Chaos, Solitons and Fractals

Nonlinear Science, and Nonequilibrium and Complex Phenomena

journal homepage: www.elsevier.com/locate/chaos

Extended detrended cross-correlation analysis of nonstationary processes

A.N. Pavlov [a,b,*], O.N. Pavlova [a], A.A. Koronovskii Jr. [a], G.A. Guyo [a,b]

[a] Saratov State University, Astrakhanskaya Str. 83, Saratov 410012, Russia
[b] Regional Scientific and Educational Mathematical Center "Mathematics of Future Technologies", 410012 Saratov, Russia

ARTICLE INFO

Article history:
Received 4 January 2022
Received in revised form 19 February 2022
Accepted 2 March 2022
Available online xxxx

Keywords:
Cross-correlation analysis
Detrended fluctuation analysis
Long-range correlations
Cerebral blood flow

ABSTRACT

We propose an extension of the detrended cross-correlation analysis (DCCA) for signals with highly inhomogeneous structure. The proposed approach evaluates two scaling exponents, one of which characterizes the detrended covariance, and the second exponent quantifies the effects of nonstationarity caused by the distribution of local fluctuations of signal profiles from the trend. Using simulated datasets produced by a system of coupled Lorenz models, we describe entrainment phenomena associated with chaotic synchronization and the role of nonstationarity in their description. The processing of experimental data related to cerebral blood flow in neighboring vessels of different size confirm the general conclusion of this study and shows the possible advantages of the proposed extension of the DCCA-method for diagnosing changes in cooperative dynamics in physiological systems, where the combined effects of dynamics, nonstationarity and noise may occur.

1. Introduction

Cross-correlations occur in the dynamics of various systems [1–3], especially if such systems consist of interacting units, and the analyzed data sets reflect the temporal behavior of these units. Networks are good examples of objects, whose cross-correlations carry important information about their complex organization that can be used to monitor or predict expected dynamics. One of the most promising areas of application for cross-correlation analysis is the recently proposed network physiology [4–8]. When dealing with physiological systems, it is necessary to take into account several features of the acquired signals. In addition to measurement noise and artifacts, time-varying dynamics produces various types of nonstationary behavior, which limits the applicability of traditional correlation analysis. This problem can be partially solved by filtering procedures, including removing a trend. However, the latter does not guarantee that the resulting signal will become stationary, because other reasons can affect the performance of the method, such as intermittent behavior, nonstationarity in the amplitude or energy of the signal. Another problem with the classical correlation function consists in its reduction for random processes, which complicates the characterization of long-term power-law correlations. To improve this characterization, a variant of the root-mean-square (rms) analysis of random walk, the detrended fluctuation analysis (DFA) was proposed [9,10] and widely used in many areas of natural science [11–17]. Its main idea consists of the building an increasing function for quantifying the fluctuations in the signal profile around the local trend, depending on the segment length. This method was also modified for the case of two nonstationary time series within the detrended cross-correlation analysis (DCCA) [18,19].

Despite successful applications of DFA in various fields of natural science, this approach assumes a fairly homogeneous structure of data sets, when the fluctuations of the signal profile around the local trend are comparable for individual segments. The latter allows us to provide time-averaging of the rms fluctuations for these segments in order to obtain a scaling exponent that quantifies long-range power-law correlations, although correlations at short or middle ranges can also be estimated. Inhomogeneity of the signal profile for transients or intermittent behavior can seriously affect the performance of the DFA and lead to misinterpretations of computational results. In an effort to account for such inhomogeneity, when the impact of some segments significantly exceeds the impact of other parts of the data, we proposed an extended DFA (EDFA) [20]. This method evaluates how the differences between rms fluctuations vary with segment length and introduces an additional scaling exponent to characterize the effect of nonstationarity in the signal. EDFA has recently been illustrated using both simulated and experimental data [21]. In particular, it allowed to reveal significant distinctions in the responses of macro- and microcerebral vessels to abrupt changes in peripheral arterial pressure [20], to improve the separation of groups of rats with different

* Corresponding author at: Saratov State University, Astrakhanskaya Str. 83, Saratov 410012, Russia.
E-mail address: pavlov.alexeyn@gmail.com (A.N. Pavlov).

https://doi.org/10.1016/j.chaos.2022.111972
0960-0779/

permeability of the blood-brain barrier [22,23] and to characterize the effects of non-rapid eye movement (NREM) sleep [24]. When dealing with fairly homogeneous processes, EDFA does not provide new information compared to the traditional DFA method. However, for inhomogeneous processes characterized by a wide distribution of local rms fluctuations of the signal profile around a local trend, EDFA can improve the separation of processes with different types of nonstationary behavior.

DFA-based methods are well suited to describe the power-law behaviors of natural systems and, in particular, biological systems where experimental data are noisy due to the existence of internal noise caused by the interaction of each biological unit with all the others present in the system (for example, simple cells or neurons in the brain) and external noise coming from the environment. Even if the system is considered within the framework of a deterministic description (e.g., chaos theory), various sources of noise, internal and external, are always present in biological and physical systems. These systems are naturally noisy and sometimes even chaotic, but always with stochasticity due to external and internal noise sources. Moreover, noise often plays a constructive role in the dynamics [25–29]. To take this circumstance into account, the analysis of such systems should be based, e.g., on stochastic differential equations (SDEs) with additional noise terms. The latter can produce small changes in dynamics if the system is considered far from bifurcation points, etc. However, noise often has a positive role, especially multiplicative one, which always occurs in physical and biological systems. In particular, the multiplicative noise source models the strong interaction of the population system (as neurons, cells, etc.) with the environment, which directly affects the population species density. Recent investigations have shown the constructive role of noise in nonlinear systems of interdisciplinary physics that are far from equilibrium, e.g. [30–37].

In this paper, we propose a modification of the EDFA for cross-correlation analysis of signals with inhomogeneous structure, namely, extended detrended cross-correlation analysis (EDCCA). This approach evaluates two scaling exponents, one related to detrended covariance as in the original work [18], and the second one describes the effects of nonstationarity caused by the distribution of local rms deviations of signal profiles from simple linear or polynomial functions describing local trends. We illustrate the EDCCA method for both simulated and experimental datasets. The paper is organized as follows. In Section 2, we describe the extended approach for detrended cross-correlation analysis and simulated/experimental data. The main results describing the potential of EDCCA in studying the nonstationary dynamics of nonlinear systems are given in Section 3. Section 4 summarizes the conclusions of the study.

2. Methods and experiments

2.1. DFA and its extended version EDFA

Detrended fluctuation analysis (DFA) [9,10] has been proposed to characterize long-range power-law correlations in various natural processes, especially, if the time series acquired are nonstationary, and the applicability of traditional correlation analysis becomes questionable. Besides nonstationarity, DFA improves the quantitative assessment of the features of power-law statistics in the region of long-range correlations for random processes, in which the correlation function decreases rapidly. The method evaluates the profile y_k of the time series x_i, $i = 1, \ldots, N$ as

$$y_k = \sum_{i=1}^{k} [x_i - \langle x \rangle], \tag{1}$$

where $\langle x \rangle$ is the mean value. Retrieving of $\langle x \rangle$ is not required at this stage and can be omitted, since this value will be taken into account during the trend removal procedure.

The profile y_k is then separated into segments of length n, and the linear local trend z_k is estimated in every segment according to the least-squares approach. Fluctuations of the profile often show a power-law dependence with the scaling exponent α

$$F_{DFA}(n) = \sqrt{\frac{1}{N}\sum_{k=1}^{N} [y_k - z_k]^2} \sim n^{\alpha}. \tag{2}$$

Some distinctions in the algorithmic procedure can be taken into account, e.g., accounting for overlapping segments, non-linear fitting of the local trend, etc., but they are not decisive for the performance of the method. The relationship between α and other characteristics describing the features of a signal is discussed in many studies, e.g. [14,15]. Using α, differences in the signal structure are quantified, in particular, the presence of anti-correlations ($\alpha < 0.5$), positive power-law correlations ($0.5 < \alpha < 1$), uncorrelated behavior ($\alpha = 0.5$), etc.

Let us now discuss the case when the nonstationarity properties differ significantly throughout the signal, and the role of some segments considerably exceeds the influence of other parts of the data. This is observed, e.g., for intermittent dynamics or transients. Thus, Fig. 1 shows two examples of significant distinctions between profile segments, where local standard deviations $F_{loc}(n)$ estimated inside segments of length n, have a broad distribution. According to Fig. 1a, the first type of nonstationarity (trend) is characterized by the largest value of F_{loc} for the first segment, and the related F_{loc} exceeds the sum of local standard deviations for the remaining parts. For the second type of nonstationarity (switching between different random processes) F_{loc} for the first segment is 30 times more than for the second.

The dominant role of several segments produces essential differences in the estimated quantities for cases when some parts of the data are included or removed. For transients, the given problem can be solved by detrending procedures (filtering low-frequency components). For other types of nonstationary behavior (intermittency, nonstationarity in amplitudes), the ways to solve the problem are more complicated. If the origin of nonstationarity is associated with the complex dynamics of the system under study, it is not always obvious whether some data segments should be excluded from the analysis.

To take into account the distinctions in local fluctuations, we proposed to consider an additional measure representing the difference between the maximum and minimum local standard deviation of the signal profile from the trend [20]

$$dF_{EDFA}(n) = \max [F_{loc}(n)] - \min [F_{loc}(n)] \tag{3}$$

or the width of the distribution of local standard deviations [38]. We call this approach extended DFA (EDFA) and analyze the power-law behavior of measure (3)

$$dF_{EDFA}(n) \sim n^{\beta}. \tag{4}$$

An example showing that α and β exponents are different quantities is illustrated in Fig. 2. Both these quantities can be useful diagnostic tools, and their simultaneous estimation can improve the analysis of physiological data sets [20,24,38].

2.2. DCCA and its extension EDCCA

In [18], a method was proposed for describing long-range cross-correlations in the nonstationary dynamics of various systems, called the detrended cross-correlation analysis (DCCA). Its main idea is the following generalization of the DFA approach. Consider two interrelated time series $\{x_i\}$ and $\{\widetilde{x}_i\}$, $i = 1, \ldots, N$, which exhibit time-varying behavior and do not satisfy the stationarity property. Their profiles (random walks) are introduced as

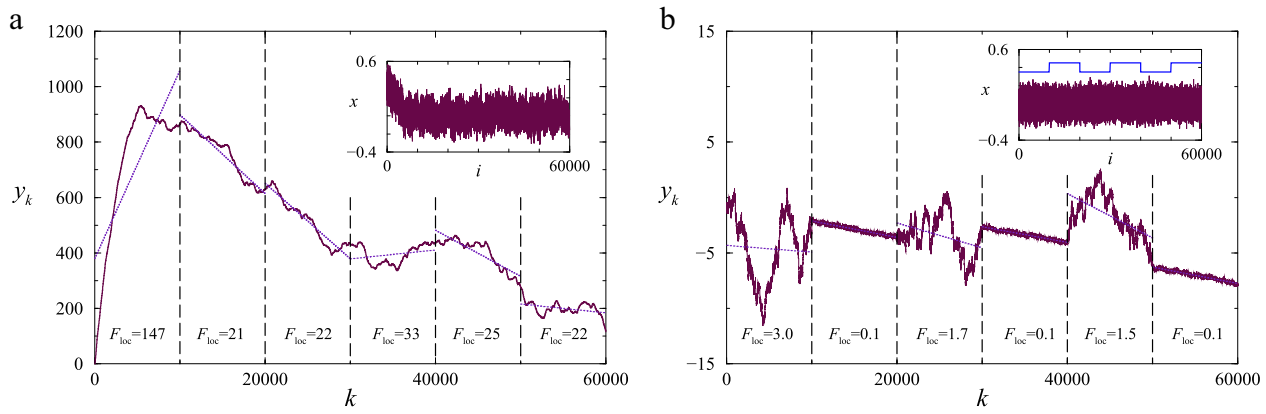

Fig. 1. Two examples of profiles for nonstationary signals x_i: floating mean value (trend) (a) and switching between white noise and noise with anticorrelations ($\alpha = 0.1$) (b). Local standard deviations are shown in each segment for $n = 10{,}000$.

$$y_k = \sum_{i=1}^{k} x_i, \quad \tilde{y}_k = \sum_{i=1}^{k} \tilde{x}_i. \tag{5}$$

Further, each profile is divided into N–n overlapping segments of $n - 1$ values, and the local trend in each segment ($i \le k \le i + n$) is estimated according to the linear least squares fit.

The detrended cross-correlation is assessed for every segment

$$f^2_{DCCA}(n,i) = \frac{1}{n-1}\sum_{k=i}^{i+n}(y_k - z_k)(\tilde{y}_k - \tilde{z}_k) \tag{6}$$

where z_k and $\tilde{z}_k$ are the related local trends, and then averaged over all available parts of data

$$F^2_{DCCA}(n) = \frac{1}{N-n}\sum_{i=1}^{N-n} f^2_{DCCA}(n,i). \tag{7}$$

When dealing with one time series ($x_i = \tilde{x}_i$), the algorithm becomes analogous to the standard DFA. In the case of long-range cross-correlations, the $F_{DCCA}(n)$ dependence exhibits a power-law behavior with the scaling exponent λ

$$F_{DCCA}(n) \sim n^{\lambda}. \tag{8}$$

In this paper, we propose an extension of the DCCA method by analogy with the EDFA approach. For two interrelated time series, in which the properties of nonstationarity vary significantly, we will take into account the variability of local fluctuations of the profiles. To do this, we propose to estimate the difference between the maximum and minimum local standard deviation of each signal profile from the trend

$$\begin{aligned} dF(n) &= \max[F_{loc}(n)] - \min[F_{loc}(n)], \\ d\tilde{F}(n) &= \max\left[\tilde{F}_{loc}(n)\right] - \min\left[\tilde{F}_{loc}(n)\right], \end{aligned} \tag{9}$$

and introduce a measure describing the effects of nonstationarity

$$dF_{EDCCA}(n) = \sqrt{dF(n) * d\tilde{F}(n)}. \tag{10}$$

This measure has often a power-law dependence, which is described by a scaling exponent other than λ

$$dF_{EDCCA}(n) \sim n^{\mu}. \tag{11}$$

For stationary processes, the measures $dF(n)$ and $d\tilde{F}(n)$ tend to zero, i.e., $dF_{EDCCA}(n)$ takes small values. In such case, the scaling exponent μ does not provide an informative characteristic of the signals, but this exponent distinguishes interrelated processes with varying degrees of inhomogeneity, which is useful in many diagnostic-related problems.

Alternatively, we can consider the widths of the probability distributions, characterized by the standard deviations

$$dF_{EDCCA}(n) = \sqrt{\sigma(F_{loc}(n)) * \sigma\left(\tilde{F}_{loc}(n)\right)} \sim n^{\mu}. \tag{12}$$

Both definitions (11) and (12) are similar, however, the latter approach can provide more stable results when dealing with inhomogeneous data sets containing, e.g., artifacts or extreme events. In Section 3 we describe examples of using the μ measure to characterize both simulated and experimental data.

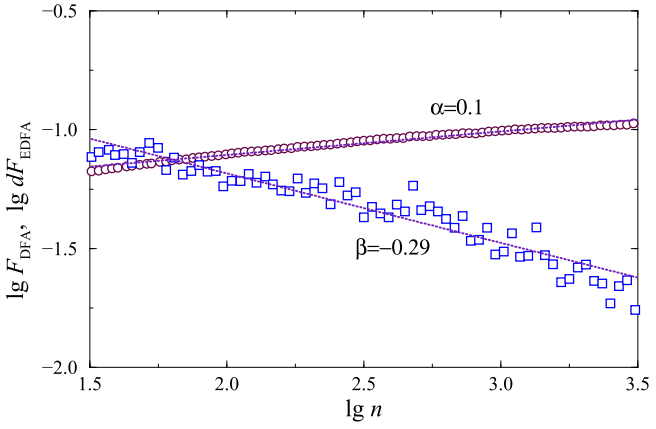

Fig. 2. An example of computing the exponents α and β for a random process with anti-correlations (derivative of 1/*f*-noise).

2.3. Simulated data

We will consider simulated datasets produced by a system of two coupled Lorenz models. The Lorenz equations are the benchmark model that is widely used to study chaotic oscillations and the mechanisms of their development [39]. Cross-correlation analysis can be applied to reveal synchronization features in interacting units described by the following six ordinary differential equations

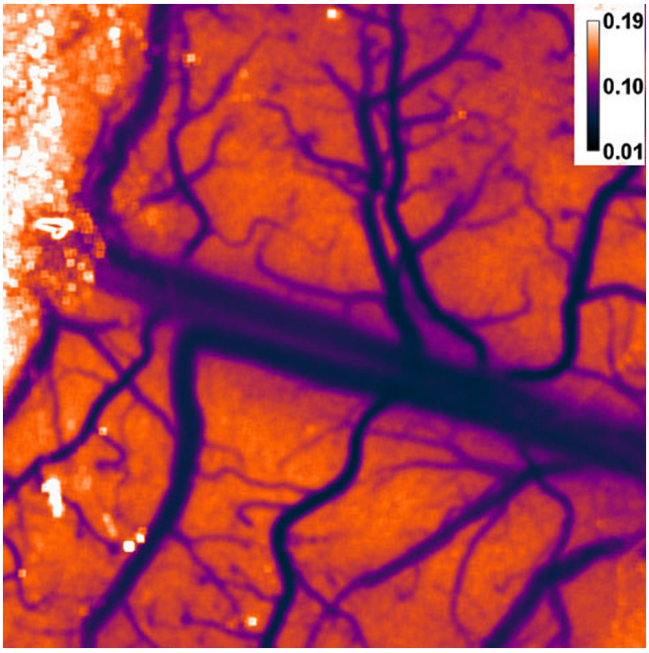

Fig. 3. An example of a speckle image of cerebral blood vessels of different sizes.

$$\begin{aligned}\frac{dx_{1,2}}{dt} &= s(y_{1,2}-x_{1,2}) + \gamma(x_{2,1}-x_{1,2}),\\ \frac{dy_{1,2}}{dt} &= r_{1,2}x_{1,2}-x_{1,2}z_{1,2}-y_{1,2},\\ \frac{dz_{1,2}}{dt} &= x_{1,2}y_{1,2}-z_{1,2}b,\end{aligned} \tag{13}$$

where the parameters $s = 10, r_1 = 28.8, r_2 = 28$, and $b = 8/3$ govern the dynamics of each subsystem, and γ is the coupling strength. The analysis of the system (13) will be carried out on the basis of series of return times into the Poincaré sections introduced as $x_1^2 + y_1^2 = 30$ and $x_2^2 + y_2^2 = 30$. The effects of nonstationarity will be considered by adding a trend to these series, which is modeled by a segment (1/4 of the period) of the cosine function. We will also consider SDEs by adding a noise term to the first equation of the second subsystem (additive white noise).

A quite atypical phenomenon demonstrated by Eq. (13) consists in the initial desynchronization [40] in the range $\gamma \in [0.0, 2.0]$. With a further increase in the coupling strength, the oscillation frequencies of both subsystems tend to be adjusted that is in accordance with the commonly expected behavior of interacting units with self-sustained oscillations.

2.4. Experimental data

As experimental data we shall consider the velocity of relative cerebral blood flow (CBF) measured in rats by means of the laser speckle contrast analysis [41–43]. The experiments were done in 8 adult male rats according to the "Guide for the Care and Use of Laboratory Animals". Before the experiment, the rats were adapted to environmental conditions for 1/2 h and then a background recording (control state) was done. Further, an injection of mesaton (Sigma) was performed at a dose 0.5 μg/kg, which produced a growth in peripheral arterial pressure, and the related recordings were done (10 min after the injection). According to physiological assumptions, such changes are not reflected in CBF due to the existing protecting mechanisms, although some reactions in the capillary network may be observed. To study these reactions, the cerebral cortex was illuminated with a He-Ne laser (Thorlabs HNL210L, 632.8 nm). Speckle patterns were acquired using a Basler acA2500-14gm CMOS camera with the sampling rate of 40 frames/s. The contrast was estimated as $K = S/\langle I\rangle$, where S and $\langle I\rangle$ are the standard deviation and mean intensity, averaged over 5×5 pixels window. The velocity of the relative CBF was estimated as a value inversely proportional to K [44] (Fig. 3). The speckle image enables to choose a focusing point inside a large vessel for temporal dynamics analysis. To study microcirculation in small surrounding vessels and measure the velocity of relative CBF in capillaries, an integral assessment of a speckle image fragment near a large vessel is carried out [45,46].

3. Results and discussion

3.1. Simulated data

Cross-correlation analysis of datasets related to both units of the system (13) makes it possible to distinguish between the states of their synchronous and asynchronous dynamics. The presence of additional nonstationarity complicates this analysis, since the behavior of the power-law dependencies (8) and (11) differs significantly from the expected results. This is illustrated in Fig. 4, where the open symbols refer to stationary chaotic oscillations, and the dotted lines show changes in the lg–lg dependencies provoked by variations in the mean value (trend) at the beginning of both datasets. According to Fig. 4, the effects of nonstationarity prevail in the region of long-range correlations ($\lg n > 2.8$ for asynchronous chaos and $\lg n > 2.3$ for synchronous chaotic oscillations), where the slopes of the dependencies become

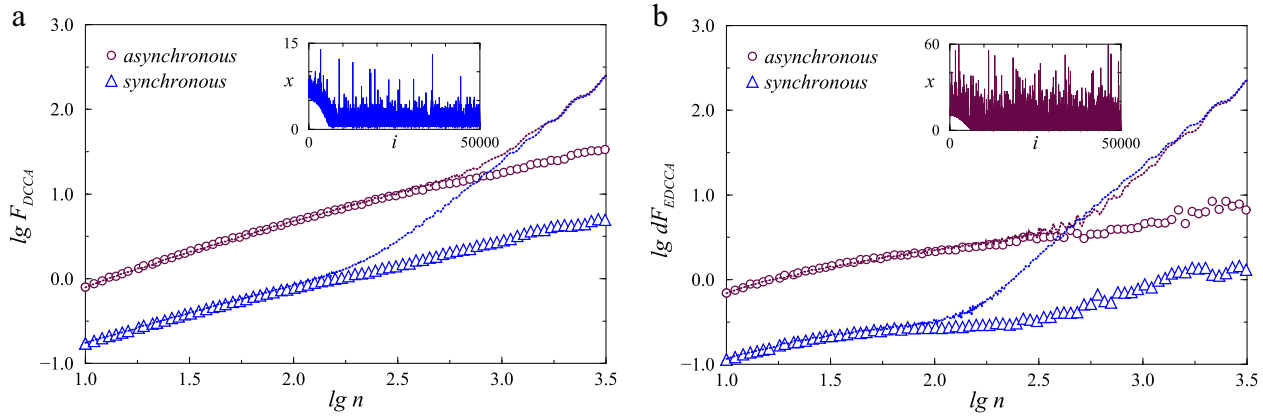

Fig. 4. Dependencies (8) and (11) in the lg–lg plot for synchronous and asynchronous dynamics of system (13). Open symbols indicate associated dependencies for stationary processes, and dotted lines show how these dependencies change when a trend is added. The insets contain signals with a trend for synchronous (a) and asynchronous (b) oscillations.

equal. Moreover, in this range of scales, we clearly obtain significantly higher scaling exponents that do not reflect the dynamical changes in return times caused by synchronization. Slope changes define the upper limit of the available scale range that can be used to study dynamical changes in system behavior which do not relate to nonstationarity effects. If this range is sufficient to estimate the scaling exponents, i.e., the distinctions in dynamics are due to short- or middle-range correlations, the datasets can be processed without pre-filtering, assuming that the slopes are estimated in a restricted region of lg$n$. Otherwise, if a wider range of scales is to be considered, a preliminary trend removal procedure becomes mandatory. Note, that this a separation of ranges is better provided based on the exponent μ, since dependencies (11) or (12) are often more sensitive to nonstationarity than (8) and changes in slopes of lgF_{DCCA} vs lg$n$ may be relatively weaker. In relation to the considered case of synchronization in system (13), the region lg$n$ < 2.2 allows one to analyze the changes in cross-correlations that occur with an increase in the coupling strength (Fig. 5). Here, for $\gamma > 6$, both interacting units show synchronous chaotic oscillations, and a further increase in γ does not change the scaling exponents. Moreover, even for the stationary dynamics of system (13) (open symbols in Fig. 4), consideration of the region of long-range correlations, e.g., lg$n$ > 3.0, becomes less informative for studying the effects of entrainments of interacting units. The considered types of oscillations are quite stable to noise, added to the system (13). Thus, for noise intensity I~10^{-4}, the results are very close to those for the deterministic system (13).

3.2. Experimental data

Analysis of physiological processes confirms the conclusions of Section 3.1. Thus, Fig. 6 shows the results of cross-correlation analysis for two adjacent vessels branched from the sagittal sinus after an acute increase in peripheral blood pressure. The inset shows an example of a time series which contains several types of nonstationary behavior. In addition to the low-frequency variation in the mean value, there are changes in amplitude (energy) and the appearance of short-term impulses or extreme events which are not observed in the beginning part of this time series. Such nonstationarity affects the power-law dependencies shown in Fig. 6 in the lg–lg plot. Again, we can clearly see changes in the slopes at lg$n$ = 2.3 that are better expressed for the lgdF_{EDCCA} vs lg$n$ dependency. The λ-exponent changes from 0.57 to 1.0, while μ increases from −0.25 to 1.85. Due to this we could expect that dynamical changes in cerebral blood vessels do not associating with the nonstationarity could be related to the region lg$n$ < 2.3. Note that changes in the dynamics of physiological systems can also be found in the region of long-range correlations, and the properties of nonstationarity can differ between distinct physiological states. Fig. 6

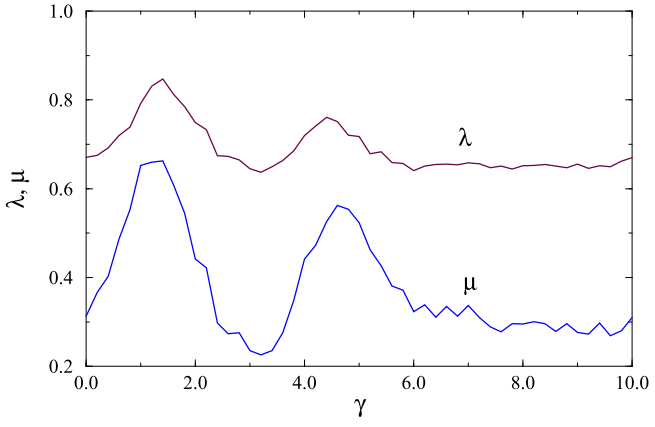

Fig. 5. Changes in the λ- and μ-exponents with increasing coupling strength in the model (13).

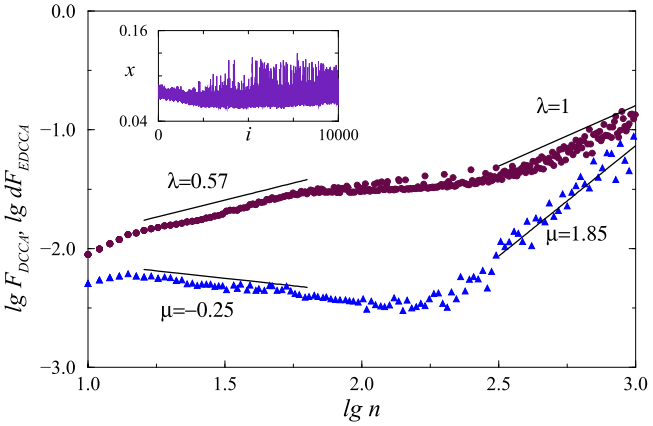

Fig. 6. Cross-correlation analysis of the relative CBF velocity in adjacent large vessels branched from the sagittal sinus after mesaton injection. The inset shows the related signal for one vessel.

shows that to characterize the dynamics of the system, it is incorrect to use a single exponent, estimated over the entire range of scales. Based on the DCCA extension, we clearly see that at least two ranges need to be considered separately, namely, lg$n$ < 2.3 and lg$n$ > 2.3. Prefiltering can reduce the effects of nonstationarity, but it does not always perform a transition to stationary datasets, especially if nonstationarity is different from trend. Therefore, consideration of the behavior of lgdF_{EDCCA} vs lg$n$ is important to choose an appropriate range of scales for comparing differences in physiological states.

After this preliminary study, let us consider in more detail the cross-correlation analysis of the dynamics of macro- and microcerebral blood flow in adjacent vessels of different sizes. The interest to this problem is caused by recent studies [47,48], which have shown that the response to abrupt changes in peripheral blood pressure can differ between large cerebral vessels and capillaries. Due to the protection mechanisms of the brain, large vessels usually do not demonstrate clear changes in their dynamics, but the reaction of the capillary network can be detected. The latter enables to expect changes in cross-correlations between the relative CBF in neighboring vessels of different sizes. Fig. 7 confirms this assumption for a group of animals. Here we considered the lg$n$ < 2.3 region and compared the cross-correlations based on the λ-exponent and two variants for computing the μ-exponent. According to Fig. 7, these exponents decrease in the considered range of scales after the injection of mesaton and the related "jump" of peripheral arterial pressure. In particular, λ changes from 0.92 ± 0.05 to 0.8 ± 0.05 (p < 0.05 according to the Mann-Whitney test), and μ reduces from 0.45 ± 0.09 to 0.17 ± 0.07 when considering definition (11) and from 0.53 ± 0.08 to 0.23 ± 0.08 (p < 0.01, the Mann-Whitney test) when using definition (12). Regardless of the definition, the μ exponent shows stronger changes compared to λ, confirming that the proposed extension of the DCCA-method can be a useful tool for diagnostics changes in physiological regulatory mechanisms caused by varying functioning conditions. The observed distinctions exceed those in the region of long-range correlation, where nonstationarity affects the estimates and pre-filtering does not improve the separation of groups compared to the results given in Fig. 7. In our opinion, the EDCCA method provides a more thorough analysis of data, taking into account the features of their structure.

4. Conclusion

Nonstationary dynamics of complex systems affects their reliable characterization from experimentally recorded datasets. In this regard, extensions of signal processing tools are often a required task to improve their diagnostic capabilities. Here, we address the problem of

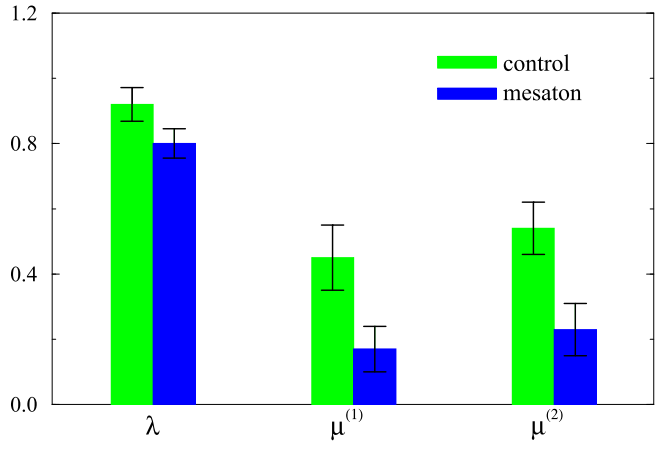

Fig. 7. Estimation of the λ and μ-exponents according to definitions (11) and (12), respectively for two states: control state and after injection of mesaton.

modifying cross-correlation analysis based on the DCCA-method. By analogy with the recently proposed EDFA, we suggest to estimate two scaling exponents, one of which is associated with DCCA and quantifies cross-correlations in interrelated time series, and the other exponent takes into account the effects of nonstationarity. The latter measure is less informative for stationary datasets and increases for processes with inhomogeneous structure. Analysis of the dependence of local rms deviations of signal profiles from trend gives an opportunity to select a suitable range of scales where power-law statistics are observed, and to avoid combining ranges with distinct scaling properties. Such approach was used to characterize the entrainment phenomena in the dynamics of coupled Lorenz models that produce chaotic oscillations. In addition to quantifying the transition from asynchronous to synchronous chaos with increasing coupling strength, we analyzed the effects of nonstationarity on this characterization. Further, we applied this approach to study cross-correlations in the dynamics of adjacent cerebral vessels and their changes caused by abrupt growth in peripheral blood pressure. The results obtained confirm the conclusions for the simulated datasets and illustrate the advantages of the proposed DCCA extension in the numerical description of pharmacologically induced changes in CBF dynamics. We hope that this tool can be useful in various studies of interactions of physiological systems, where combined effects of dynamics and nonstationary behavior are observed, e.g., in network physiology.

CRediT authorship contribution statement

A.N. Pavlov: Conceptualization, Methodology, Writing – review & editing, Supervision. **O.N. Pavlova:** Investigation, Writing – original draft. **A.A. Koronovskii:** Software, Investigation. **G.A. Guyo:** Formal analysis, Investigation, Visualization, Validation.

Declaration of competing interest

The authors declare that they have no known competing financial interests or personal relationships that could have appeared to influence the work reported in this paper.

Acknowledgments

The authors acknowledge O.V. Semyachkina-Glushkovskaya and A.S. Abdurashitov for their interest to this work and valuable discussions. This work was supported by the Russian Science Foundation (Agreement 22-22-00065) in the part of theoretical studies and numerical analysis, and the grant of the Government of the Russian Federation No. 075-15-2019-1885 in the part of physiological experiments.

References

[1] Campillo M, Paul A. Long-range correlations in the diffuse seismic coda. Science. 2003;299:547–9.
[2] Samuelsson P, Sukhorukov EV, Büttiker M. Orbital entanglement and violation of bell inequalities in mesoscopic conductors. Phys Rev Lett. 2003.;91:157002.
[3] Neder I, Heiblum M, Mahalu D, Umansky V. Entanglement, dephasing, and phase recovery via cross-correlation measurements of electrons. Phys Rev Lett. 2007.; 98:036803.
[4] Bashan A, Bartsch RP, Kantelhardt JW, Havlin S, Ivanov PCh. Network physiology reveals relations between network topology and physiological function. Nat Commun. 2012;3:702.
[5] Bartsch RP, Liu KKL, Bashan A, Ivanov PC. Network physiology: how organ systems dynamically interact. PLoS One. 2015.;10:e0142143.
[6] Ivanov PC, Liu KKL, Bartsch RP. Focus on the emerging new fields of network physiology and network medicine. New J Phys. 2016.;18:100201.
[7] Moorman JR, Lake DE, Ivanov PCh. Early detection of sepsis – a role for network physiology? Crit Care Med. 2016;44:e312–3.
[8] Rizzo R, Zhang X, Wang JWJL, Lombardi F, Ivanov PCh. Network physiology of cortico-muscular interactions. Front Physiol. 2020.;11:558070.
[9] Peng CK, Buldyrev SV, Havlin S, Simons M, Stanley HE, Goldberger AL. Mosaic organization of DNA nucleotides. Phys Rev E. 1994;49:1685–9.
[10] Peng CK, Havlin S, Stanley HE, Goldberger AL. Quantification of scaling exponents and crossover phenomena in nonstationary heartbeat time series. Chaos. 1995;5: 82–7.
[11] Buldyrev SV, Goldberger AL, Havlin S, Mantegna RN, Matsa ME, Peng CK, Simons M, Stanley HE. Long-range correlation properties of coding and noncoding DNA sequences: GenBank analysis. Phys Rev E. 1995;51:5084–91.
[12] Ivanova K, Ausloos M. Application of the detrended fluctuation analysis (DFA) method for describing cloud breaking. PhysA. 1999;274:349–54.
[13] Stanley HE, Amaral LAN, Goldberger AL, Havlin S, Ivanov PCh, Peng CK. Statistical physics and physiology: monofractal and multifractal approaches. PhysA. 1999; 270:309–24.
[14] Talkner P, Weber RO. Power spectrum and detrended fluctuation analysis: application to daily temperatures. Phys Rev E. 2000;62:150–60.
[15] Heneghan C, McDarby G. Establishing the relation between detrended fluctuation analysis and power spectral density analysis for stochastic processes. Phys Rev E. 2000;62:6103–10.
[16] Ma QDY, Bartsch RP, Bernaola-Galván P, Yoneyama M, Ivanov PCh. Effect of extreme data loss on long-range correlated and anticorrelated signals quantified by detrended fluctuation analysis. Phys Rev E. 2010.;81:031101.
[17] Frolov NS, Grubov VV, Maksimenko VA, Lüttjohann A, Makarov VV, Pavlov AN, Sitnikova E, Pisarchik AN, Kurths J, Hramov AE. Statistical properties and predictability of extreme epileptic events. Sci Rep. 2019;9:7243.
[18] Podobnik B, Stanley HE. Detrended cross-correlation analysis: a new method for analyzing two nonstationary time series. Phys Rev Lett. 2008.;100:084102.
[19] Podobnik B, Grosse I, Horvatić D, Ilic S, Ivanov PCh, Stanley HE. Quantifying cross-correlations using local and global detrending approaches. Eur Phys J B. 2009;71: 243.
[20] Pavlov AN, Abdurashitov AS, Koronovskii Jr AA, Pavlova ON, Semyachkina-Glushkovskaya OV, Kurths J. Detrended fluctuation analysis of cerebrovascular responses to abrupt changes in peripheral arterial pressure in rats. Commun Nonlin Sci Numer Simulat. 2020.;85:105232.
[21] Pavlov AN, Pavlova ON, Semyachkina-Glushkovskaya OV, Kurths J. Extended detrended fluctuation analysis: effects of nonstationarity and application to sleep data. Eur Phys J Plus. 2021;136:10.
[22] Pavlov AN, Khorovodov AP, Mamedova AT, Koronovskii Jr AA, Pavlova ON, Semyachkina-Glushkovskaya OV, Kurths J. Changes in blood-brain barrier permeability characterized from electroencephalograms with a combined wavelet and fluctuation analysis. Eur Phys J Plus. 2021;136:577.
[23] Pavlov AN, Dubrovsky AI, Koronovskii Jr AA, Pavlova ON, Semyachkina-Glushkovskaya OV, Kurths J. Extended detrended fluctuation analysis of sound-induced changes in brain electrical activity. ChaosSolitonsFractals. 2021.; 139:109989.
[24] Pavlov AN, Dubrovsky AI, Koronovskii Jr AA, Pavlova ON, Semyachkina-Glushkovskaya OV, Kurths J. Extended detrended fluctuation analysis of electroencephalograms signals during sleep and the opening of the blood-brain barrier. Chaos. 2020.;30:073138.
[25] Mikhaylov A, Pimashkin A, Pigareva Y, Gerasimova S, Gryaznov E, Shchanikov S, Zuev A, Talanov M, Lavrov I, Demin V, Erokhin V, Lobov S, Mukhina I, Kazantsev V, Wu H, Spagnolo B. Neurohybrid memristive CMOS-integrated systems for biosensors and neuroprosthetics. Front Neurosci. 2020;14:358.
[26] Chichigina O, Valenti D, Spagnolo B. A simple noise model with memory for biological systems. Fluct Noise Lett. 2005;5:L243–50.
[27] Surazhevsky IA, Demin VA, Ilyasov AI, Emelyanov AV, Nikiruy KE, Rylkov VV, Shchanikov SA, Bordanov IA, Gerasimova SA, Guseinov DV, Malekhonova NV, Pavlov DA, Belov AI, Mikhaylov AN, Kazantsev VB, Valenti D, Spagnolo B, Kovalchuk MV. Noise-assisted persistence and recovery of memory state in a memristive spiking neuromorphic network. ChaosSolitonsFractals. 2021.; 146:110890.
[28] Ushakov YuV, Dubkov AA, Spagnolo B. Regularity of spike trains and harmony perception in a model of the auditory system. Phys Rev Lett. 2011.;107:108103.
[29] YuV Ushakov, Dubkov AA, Spagnolo B. Spike train statistics for consonant and dissonant musical accords in a simple auditory sensory model. Phys Rev E. 2010.; 81:041911.

[30] Denaro G, Valenti D, Spagnolo B, Basilone G, Mazzola S, Zgozi SW, Aronica S, Bonanno A. Dynamics of two picophytoplankton groups in Mediterranean sea: analysis of the deep chlorophyll maximum by a stochastic advection-reaction-diffusion model. PLoS One. 2013.;8:e66765.
[31] Guarcello C, Valenti D, Spagnolo B. Phase dynamics in graphene-based Josephson junctions in the presence of thermal and correlated fluctuations. Phys Rev B. 2015.;92:174519.
[32] Caruso A, Gargano ME, Valenti D, Fiasconaro A, Spagnolo B. Cyclic fluctuations, climatic changes and role of noise in planktonic foraminifera in the Mediterranean Sea. Fluct Noise Lett. 2005;5:L349–55.
[33] Guarcello C, Valenti D, Spagnolo B, Pierro V, Filatrella G. Anomalous transport effects on switching currents of graphene-based Josephson junctions. Nanotechnology. 2017.;28:134001.
[34] Carollo A, Valenti D, Spagnolo B. Geometry of quantum phase transitions. Phys Rep. 2020;838:1–72.
[35] Guarcello C, Valenti D, Carollo A, Spagnolo B. Stabilization effects of dichotomous noise on the lifetime of the superconducting state in a long Josephson junction. Entropy. 2015;17:2862–75.
[36] Carollo A, Spagnolo B, Valenti D. Uhlmann curvature in dissipative phase transitions. Sci Rep. 2018;8:9852.
[37] Yakimov AV, Filatov DO, Gorshkov ON, Antonov DA, Liskin DA, Antonov IN, Belyakov AV, Klyuev AV, Carollo A, Spagnolo B. Measurement of the activation energies of oxygen ion diffusion in yttria stabilized zirconia by flicker noise spectroscopy. Appl Phys Lett. 2019.;114:253506.
[38] Pavlov AN, Dubrovskii AI, Pavlova ON, Semyachkina-Glushkovskaya OV. Effects of sleep deprivation on the brain electrical activity in mice. ApplSci(Basel). 2021;11:1182.
[39] Lorenz EN. Deterministic nonperiodic flow. J Atmos Sci. 1963;20:130–41.
[40] Anishchenko VS, Silchenko AN, Khovanov IA. Synchronization of switching processes in coupled Lorenz systems. Phys Rev E. 1998;57:316.
[41] Briers JD, Webster S. Laser speckle contrast analysis (LASCA): a non-scanning, full-field technique for monitoring capillary blood flow. J Biomed Opt. 1996;1:174–9.
[42] Boas DA, Dunn AK. Laser speckle contrast imaging in biomedical optics. J Biomed Opt. 2010.;15:011109.
[43] Briers D, Duncan DD, Hirst E, Kirkpatrick SJ, Larsson M, Steenbergen W, Stromberg T, Thompson OB. Laser speckle contrast imaging: theoretical and practical limitations. J Biomed Opt. 2013.;18:066018.
[44] Kazmi SS, Faraji E, Davis MA, Huang YY, Zhang XJ, Dunn AK. Flux or speed? Examining speckle contrast imaging of vascular flows. Biomed Opt Express. 2015;6:2588–608.
[45] Dunn AK. Laser speckle contrast imaging of cerebral blood flow. Ann Biomed Eng. 2012.;40:367377.
[46] Abdurashitov AS, Lychagov VV, Sindeeva OA, Semyachkina-Glushkovskaya OV, Tuchin VV. Histogram analysis of laser speckle contrast image for cerebral blood flow monitoring. Front Optoelectron. 2015;8:187–94.
[47] Pavlov AN, Semyachkina-Glushkovskaya OV, Pavlova ON, Abdurashitov AS, Shihalov GM, Rybalova EV, Sindeev SS. Multifractality in cerebrovascular dynamics: an approach for mechanisms-related analysis. ChaosSolitonsFractals. 2016;91:210–3.
[48] Pavlov AN, Abdurashitov AS, Sindeeva OA, Sindeev SS, Pavlova ON, Shihalov GM, Semyachkina-Glushkovskaya OV. Characterizing cerebrovascular dynamics with the wavelet-based multifractal formalism. PhysA. 2016;442:149–55.